Laser-induced excited state and ultrasonic wave gratings: Amplitude and phase grating contributions to diffraction

Keith A. Nelson,[a] Roger Casalegno,[b] R. J. Dwayne Miller, and M. D. Fayer

Department of Chemistry, Stanford University, Stanford, California 94305
(Received 8 February 1982; accepted 23 April 1982)

A detailed analysis of diffraction from laser-induced gratings is presented. The changes which occur in both the real and imaginary parts of the index of refraction are accounted for when excited states are created. These lead to phase and amplitude grating contributions, respectively, to the diffraction from a laser-induced excited state grating. Experimental confirmation of the predicted wavelength dependence of these contributions is presented. Diffraction from laser-induced excited state gratings, ultrasonic wave gratings, and mixed excited state and acoustic gratings is analyzed with the phase and amplitude contributions to each accounted for. The results permit the interpretation of mixed grating data and predict conditions under which density-dependent absorption spectral shifts and excited state-phonon interactions can be measured.

I. INTRODUCTION

In recent years, the results of a number of laser-induced grating experiments have been reported.[1] In a typical experiment, two time-coincident laser pulses of the same frequency are crossed inside a solid or liquid sample to set up an optical interference pattern. Light absorption leads to a spatially periodic sinuosoidal distribution of excited states, and since the optical properties of the excited states are different from those of the ground states, the excited state concentration distribution acts as a Bragg diffraction grating. This is probed by a third laser pulse (or by cw laser light) incident at the appropriate angle for diffraction (see Fig. 1). The time dependence of diffracted intensity provides information about the dynamic properties of the system. For example, in a simple system the excited state lifetime can be obtained from the rate of decay of the grating's diffracting power. Transient grating experiments have been used to measure electronic excited state energy transport,[2] trapping and relaxation rates,[3] fluorescence quantum yields,[4] orientational relaxation times,[5] and thermal and mass diffusion rates.[6]

The transient grating experimental arrangement has also been used for the optical generation of ultrasonic waves.[6-9] If absorption of the excitation pulses is followed by rapid radiationless relaxation, a spatially periodic temperature distribution is produced and thermal expansion launches ultrasonic waves whose wavelength and orientation match those of the grating pattern. The waves can be detected by Bragg diffraction, since the optical properties of a system are density dependent. Thus, diffracted signals in a transient grating experiment can arise from an excited state concentration grating, an ultrasonic wave grating, or a combination of the two. Laser-induced ultrasonic waves have been used to measure crystal elastic constants,[7] second sound propagation,[10] and overtone absorption spectra.[11] It was recently demonstrated that transient grating optical excitation of ultrasonic waves is possible in transparent samples.[9] In this case, stimulated Brillouin scattering (electrostriction) couples the crossed laser excitation pulses to the material acoustic field. This phenomenon has been used to measure photoelastic constants.[11]

In most analyses of crossed-laser experiments involving excited state concentration gratings, diffraction has been attributed entirely to amplitude grating effects[12,16]—i.e., to the spatially periodic variation in the optical density D. Typically, the probe is absorbed by one species, for example, the ground state, and absorbed weakly or not at all by the excited state. The intensity of the diffracted signal η_a due to amplitude grating effects alone is proportional to the square of the grating's peak–null difference in optical density[13]:

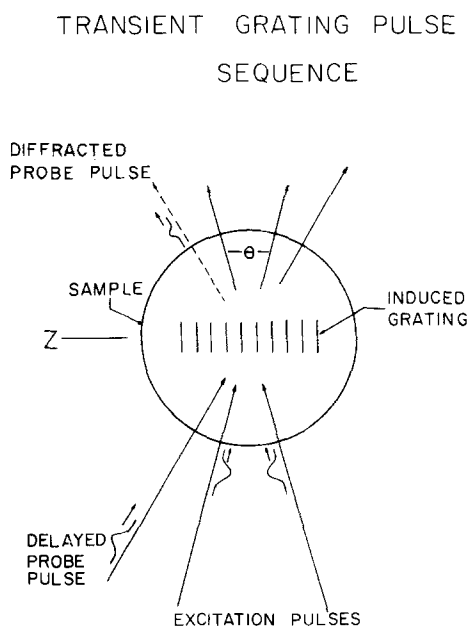

FIG. 1. Schematic illustration of the transient grating experiment. Interference between the incoming excitation pulses results in an oscillatory density of excited states, which Bragg diffracts the subsequent probe pulse. Acoustic waves are generated which propagate in the direction of the grating wave vector (the z axis). The grating wavelength is given by $\Lambda = \lambda / 2\sin(\theta/2)$, where λ is the excitation wavelength in air.

[a] Permanent address: Chemistry Department, MIT, Cambridge, Mass. 02139.

[b] Permanent address: Laboratoire de Spectrométrie Physique, Université I, 38041 Grenoble, France.

 0021-9606/82/151144-09$02.10

$$\eta_a = a[D(\text{peak}) - D(\text{null})]^2 \equiv a(\Delta D)^2 , \quad (1)$$

where a is the amplitude grating proportionality constant.

As is well known from diffraction theory in optics and holography, a volume grating's diffracting power depends not only on the peak–null variation in D, i.e., in the imaginary part of the refractive index, but also on the variation in n, the real part of the refractive index. Thus, the total diffraction η is a sum of amplitude and phase grating contributions[13]

$$\eta = \eta_a + \eta_p = a(\Delta D)^2 + b(\Delta n)^2 , \quad (2)$$

where η_p is the diffracted intensity due to phase grating effects, Δn is the grating's peak–null difference in n, and b is the phase grating proportionality constant. For an excited state concentration grating, regardless of the magnitude of ΔD, the second term in Eq. (2) is comparable to or larger than the first. Thus, the phase grating contribution to the total diffracted intensity cannot be ignored. Its omission can lead to erroneous interpretations of transient grating data.

In this paper, we examine the influence of excited state phase grating effects on transient grating experimental results. We present experimental observations of excited state phase grating diffraction which are in accord with the theoretical predictions. Special attention is paid to the influence of phase grating effects on diffraction from mixed excited state and ultrasonic wave gratings. In earlier work,[7,8] the neglect of excited state phase grating effects led to misinterpretation of the ultrasonic wave grating (acoustic grating) diffraction. The experimental conditions under which acoustic amplitude grating diffraction could be observed are also predicted. Such observations would be of value[7,8] since they would allow direct measurement of excited state–phonon interactions and excited state intermolecular interactions.

II. THEORY

In this section, we calculate the phase and amplitude contributions to diffraction from an excited state grating, an acoustic grating, and a mixed grating as a function of probe wavelength. We assume the following throughout. The crossed excitation pulses produce a sinusoidal optical interference pattern whose intensity is not diminished through the depth of the sample. (The excitation pulses are not significantly depleted as they pass through the sample.) The grating wave vector is parallel to the front and rear surfaces of the sample (the grating is not "slanted"). The sample thickness is T. The probe beam, of frequency ω and wavelength λ in air, is incident on the sample at the Bragg angle θ. (Deviations from θ decrease the overall diffraction efficiency, but the relative phase and amplitude contributions are unaffected.)

The grating's diffraction properties will be described in terms of the complex index of refraction $\tilde{n}$, where

$$\tilde{n} = n + ik . \quad (3)$$

The imaginary (absorptive) part of $\tilde{n}$ is related to the optical density D by

$$D = 4\pi Tk/2.3\lambda . \quad (4)$$

We assume throughout that $k \ll 1$, which is the case except for extremely intense absorption bands. For a sinusoidal volume grating, the diffraction efficiency η is[13]

$$\eta(\omega) = \exp\left[-\frac{2.3 D_{av}(\omega)}{\cos\theta}\right]\left[\sinh^2\frac{\pi\Delta k(\omega)T}{\lambda\cos\theta} + \sin^2\frac{\pi\Delta n(\omega)T}{\lambda\cos\theta}\right]$$
$$= \eta_a(\omega) + \eta_p(\omega) , \quad (5)$$

where $\Delta k(\omega)$ and $\Delta n(\omega)$ are the gratings peak–null differences in k and n, respectively. The first term in the brackets determines the amplitude grating diffraction $\eta_a(\omega)$ and the second determines the phase grating diffraction $\eta_p(\omega)$. $D_{av}(\omega)$ is an average optical density adjusted such that the exponential term describes the absorptive loss. In most experimental situations, the total diffraction efficiency is low ($\eta < 0.01$), so Eq. (5) can be approximated by

$$\eta(\omega) = \exp\left[-\frac{2.3 D_{av}(\omega)}{\cos\theta}\right]\left(\frac{\pi T}{\lambda\cos\theta}\right)^2$$
$$\times\{[\Delta k(\omega)]^2 + [\Delta n(\omega)]^2\} , \quad (6)$$

from which Eq. (2) was written.

The optical properties of the system, i.e., $\Delta k(\omega)$ and $\Delta n(\omega)$, must now be related to the excited state concentrations and acoustic strains produced by transient grating excitation. This is accomplished by describing the system with a damped harmonic oscillator model in which the dispersion is given by[14]

$$\tilde{n}^2 - 1 = \sum_j \frac{N_j f_j'}{\omega_j^2 - \omega^2 - i\gamma_j\omega} = \sum_j \tilde{n}_j' , \quad (7)$$

where N_j is the number density of molecules in the initial state of the jth transition, ω_j and γ_j are the absorption maximum and linewidth (FWHH), and f_j' measures the absorption strength

$$f_j' = \frac{4\pi e^2}{m} f_j = \frac{8\pi}{c^2}\int_{j\text{th band}} \frac{\sigma(\lambda)d\lambda}{\lambda^2} , \quad (8)$$

where f_j is the oscillator strength,[15] σ is the absorption cross section, and e and m are the electron charge and mass, respectively. In Eq. (7), the terms $\tilde{n}_j'$ represent the contributions of the jth absorption band to the complex index of refraction. Equation (7) is appropriate for condensed phases such that the condensed-phase (rather than isolated molecule) values of ω_j and γ_j should be used. Optical anisotropy has been neglected since it introduces no essentially new effects. It could easily be considered by writing the index of refraction in the correct tensor form. Separating Eq. (7) into its real and imaginary parts gives (for $k \ll 1$)

$$n^2 - 1 = \sum_j \frac{N_j f_j'(\omega_j^2 - \omega^2)}{(\omega_j^2 - \omega^2)^2 + \gamma_j^2\omega^2} = \sum_j n_j' \quad (9)$$

and

$$2nk = \sum_j \frac{N_j f_j'\gamma_j\omega}{(\omega_j^2 - \omega^2)^2 + \gamma_j^2\omega^2} = \sum_j k_j' , \quad (10)$$

where n_j' and k_j' represent the contributions of the jth absorption band to n and k, respectively.

From Eqs. (9) and (10), the variations in optical properties (Δn and Δk) as functions of excited state populations and material strains can be calculated. Then, Eq. (6) can be used to calculate the amplitude and phase contributions to diffraction from excited state gratings, acoustic gratings, and mixed gratings.

Equations (9) and (10) give

$$\frac{dn}{dx}=\frac{1}{2n_0}\frac{d}{dx}\sum_j n_j' \tag{11}$$

and

$$\frac{dk}{dx}=\frac{1}{2n_0}\frac{d}{dx}\sum_j k_j'-\frac{1}{n_0}\left(\frac{dn}{dx}\right)\sum_j k_j' , \tag{12}$$

where x is any parameter (e.g., excited state concentration or material strain) on which the optical properties depend. n_0 is the unperturbed value of n. The second term on the right-hand side of Eq. (12) is negligible if both $k \ll 1$ and $(dn/dx) \ll 1$, as is generally the case.

To simplify the following discussion, we will consider the specific case of a guest–host system in which the probe frequency ω lies within the guest $S_0 \rightarrow S_1$ origin (i.e., $\omega \approx \omega_0$), and the origin is spectrally isolated from all other transitions (including transitions originating from the S_1 state). This is relevant to the experiments which follow, and is easily generalized to treat other situations. In this case, the origin contributions n_0' and k_0' play predominant roles in determining the optical response to excited state creation or strain. Often all other contributions can be neglected, and when this is so Eqs. (11) and (12) simplify to

$$\frac{dn}{dx}=\frac{1}{2n_0}\frac{dn_0'}{dx}=\frac{1}{2n_0}\frac{d}{dx}\left\{\frac{2N_0 f_0'(\omega_0-\omega)}{\omega_0[4(\omega_0-\omega)^2+\gamma_0^2]}\right\} \tag{13}$$

and

$$\frac{dk}{dx}=\frac{1}{2n_0}\frac{dk_0'}{dx}=\frac{1}{2n_0}\frac{d}{dx}\left\{\frac{N_0 f_0'\gamma_0}{\omega_0[4(\omega_0-\omega)^2+\gamma_0^2]}\right\} . \tag{14}$$

The second term on the right-hand side of Eq. (12) has been omitted in Eq. (14). The assumption $\omega_0 \gg (\omega_0-\omega)$ has been made, although the following calculations would be straightforward without it.

A. Excited state gratings

Only $n_0'(\omega)$ and $k_0'(\omega)$ are significantly affected by the excitation of guest molecules for $\omega \approx \omega_0$. If the number density of guest molecules in the unperturbed sample is N_0, and the number density of excited states at the grating peaks is N_1, then the grating peak–null variations $\Delta n_{ex}(\omega;N_1)$ and $\Delta k_{ex}(\omega;N_1)$ are

$$\Delta n_{ex}(\omega;N_1)=\frac{dn}{dN_0}\Delta N_0=-\frac{N_1}{N_0}\frac{2(\omega_0-\omega)}{\gamma_0}k_0(\omega) \tag{15}$$

and

$$\Delta k_{ex}(\omega;N_1)=\frac{dk}{dN_0}\Delta N_0=-\frac{N_1}{N_0}k_0(\omega) , \tag{16}$$

where $k_0(\omega)$ is the value of k for $\omega \approx \omega_0$, i.e.,

$$k_0(\omega)=k(\omega\approx\omega_0)=\frac{1}{2n_0}\frac{N_0 f_0'\gamma_0}{\omega_0[4(\omega_0-\omega)^2+\gamma_0^2]}$$

$$=\frac{k_0(\omega_0)\gamma_0^2}{4(\omega_0-\omega)^2+\gamma_0^2} , \tag{17}$$

and $k_0(\omega_0)$ the absorption maximum is

$$k_0(\omega_0)=\frac{1}{2n_0}\frac{N_0 f_0'}{\gamma_0\omega_0} . \tag{18}$$

From Eqs. (6) and (15)–(18), the excited state grating diffraction efficiency η_{ex} takes the simple form

$$\eta_{ex}(\omega)=\exp\left[-\frac{2.3D_{av}(\omega)}{\cos\theta}\right]\left[\frac{\pi T(N_1/N_0)}{\lambda\cos\theta}\right]^2 k_0(\omega_0)k_0(\omega) . \tag{19}$$

Equations (15), (16), and (19) give the excited state grating's diffraction efficiency, and its amplitude and phase contributions. The following features should be noted.

(1) The relative amplitude and phase contributions depend only on the probe frequency ω relative to the absorption peak ω_0 and the linewidth γ_0. They *do not* depend on the strength of the absorption, and thus the phase contribution cannot be neglected for any transition in any material.

(2) At the absorption maximum the phase contribution vanishes, i.e., $\Delta n_{ex}(\omega_0)=0$. Thus, the phase grating effects can be eliminated by tuning the probe to this frequency.

(3) At the half-widths, the phase term $\Delta n_{ex}(\omega_0\pm\gamma_0/2)$ is at its largest and is equal in magnitude to the amplitude term $\Delta k_{ex}(\omega_0\pm\gamma_0/2)$. At these frequencies, the phase and amplitude contributions are equal. At frequencies closer to the absorption peak, the amplitude contribution is greater than the phase contribution; at frequencies farther from the origin, the phase contribution is greater.

(4) If absorptive loss [the exponential term in Eq. (19)] is small, the diffraction efficiency simply follows the absorption line shape $k_0(\omega)$. If only amplitude grating effects were present, diffraction efficiency would be proportional to the square of the absorption strength, leading to a sharply peaked frequency dependence. Thus, the phase contribution can be measured by experimentally determining $\eta_{ex}(\omega)$. Results of such experiments are presented below.

(5) If absorptive loss is large, then diffraction efficiency decreases at the absorption peak, leading to an "M"-shaped frequency dependence for $\eta_{ex}(\omega)$. This frequency dependence has been observed,[16] although we note that it could arise even in the absence of phase grating effects.

B. Acoustic gratings

Diffraction from an ultrasonic wave grating can in principle arise from two distinct mechanisms: (1) changes in the number density of molecules N_j and (2) changes in the positions of the resonances ω_j (density-dependent spectral shifts). Both of these affect the optical properties [described by Eqs. (9) and (10)] and

both could result in amplitude and phase grating diffraction. Under most conditions, phase grating diffraction due to changes in number density predominates, and, in fact, this probably accounts for all acoustic diffraction devices and experiments realized thus far. However, it appears that spectral shift effects could be observed under the proper circumstances. This will be discussed further in Sec. V.

(1). The effects of changes in number density are easily calculated. The acoustic strain S causes a change in number density δN given by

$$S = \delta N/N \,, \tag{20}$$

where N is the unperturbed number density. The value of $n(\omega)$ is affected by all of the absorption bands, even for $\omega \approx \omega_0$, and to calculate the effect of strain-induced changes in number density on n, Eq. (11) must be used. Since all the N_j are affected similarly by strain [i.e., Eq. (20) holds for any N_j of guest or host], Eq. (9) gives

$$\Delta n_S(\omega;\delta N) = \frac{dn}{dN}\Delta N = -\Delta S\,\frac{(n_0^2-1)}{2n_0} \,, \tag{21}$$

where ΔN and ΔS are the grating's peak–null differences in number density and strain, respectively. We note that strain-dependent variation in n is usually expressed in terms of the photoelastic constant p as[17]

$$\Delta n = -\tfrac{1}{2} p S n^3 \,. \tag{22}$$

Typical values of p are between 0.1 and 0.3,[17] giving results similar to Eq. (21). Note that $\Delta n_S(\omega;\delta N) \approx -\Delta S$.

The value of $k(\omega \approx \omega_0)$ is affected only by the origin, so Eq. (14) can be used to calculate the effect of strain-induced changes in number density on k:

$$\Delta k_S(\omega;\delta N) = \frac{dk}{dN_0}\Delta N_0 = -\Delta S k_0(\omega) \,. \tag{23}$$

Note that for normal values of k ($k \ll 1$), this is far smaller than $\Delta n_S(\omega;\delta N)$.

(2). The effects of strain-dependent spectral shifts on n and k can be derived from Eqs. (13) and (14), since only shifts in the origin band (i.e., in ω_0) will be significant for $\omega \approx \omega_0$. We assume that the position of ω_0 varies linearly with strain for the small acoustic strains applied in transient grating experiments; the peak–null difference in ω_0 is then

$$\Delta\omega_0 = \phi \Delta S \,, \tag{24}$$

where ϕ measures the interaction between the acoustic phonon and the electronic energy level. Equations (13) and (14) give

$$\Delta n_{S'}(\omega;\Delta\omega_0) = \frac{dn}{d\omega_0}\Delta\omega_0 = \frac{2\phi\Delta S[\gamma_0^2 - 4(\omega_0-\omega)^2][k_0(\omega)]^2}{\gamma_0^3 k_0(\omega_0)} \tag{25}$$

and

$$\Delta k_{S'}(\omega;\Delta\omega_0) = -\frac{8\phi\Delta S(\omega_0-\omega)[k_0(\omega)]^2}{k_0(\omega_0)\gamma_0^2} \,. \tag{26}$$

The total acoustic grating diffraction efficiency η_{ac} can now be calculated from Eq. (6), giving

$$\eta_{ac}(\omega;S) = \exp\left[-\frac{2.3 D_{av}(\omega)}{\cos\theta}\right]\left(\frac{\pi T}{\lambda\cos\theta}\right)^2 \times[(\Delta k_S + \Delta k_{S'})^2 + (\Delta n_S + \Delta n_{S'})^2] \,. \tag{27}$$

The terms inside the brackets are defined by Eqs. (21), (23), (25), and (26). We note that all four terms depend linearly on strain, so the overall dependence of acoustic grating diffraction efficiency on strain (i.e., on acoustic wave amplitude) is quadratic. We have already seen that for transitions with $k \ll 1$, $\Delta k_S(\omega;\delta N) \ll \Delta n_S(\omega;\delta N)$. Under most circumstances, the general spectral shift terms $\Delta k_{S'}$ and $\Delta n_{S'}$ are also negligible compared to Δn_S, and so diffraction from acoustic gratings arises entirely from phase grating effects due to changes in number density. This will be discussed in detail, in connection with numerical calculations, in Sec. V. It will also be shown that the spectral shift contributions should be observable under the appropriate conditions

C. Mixed excited state and acoustic gratings

The total diffraction efficiency η_m from a mixed grating can now be calculated from Eq. (6):

$$\eta_m(\omega) = \exp\left[-\frac{2.3 D_{av}}{\cos\theta}\right]\left(\frac{\pi T}{\lambda\cos\theta}\right)^2 \times[(\Delta k_{ex} + \Delta k_S + \Delta k_{S'})^2 + (\Delta n_{ex} + \Delta n_S + \Delta n_{S'})^2] \,, \tag{28}$$

where the terms in the brackets are defined by Eqs. (15), (16), (21), (23), (25), and (26). In all mixed grating experiments done to date, only the contributions of the first, fourth, and fifth terms have been observed. It will be useful to write the observed diffraction efficiency due to these terms $\eta_{obs}(\omega)$ explicitly:

$$\eta_{obs}(\omega) = \exp\left[-\frac{2.3 D_{av}(\omega)}{\cos\theta}\right]\left(\frac{\pi T}{\lambda\cos\theta}\right)\left\{\left[\frac{N_1}{N_0} k_0(\omega)\right]^2 + \left[\frac{N_1}{N_0}\frac{2(\omega_0-\omega)}{\gamma_0} k_0(\omega) + \frac{\Delta S(n_0^2-1)}{2n_0}\right]^2\right\} \,. \tag{29}$$

This expression will be used to analyze data from mixed grating experiments (Sec. V).

III. EXPERIMENTAL

Transient grating experiments were performed to measure $\eta_{ex}(\omega)$, the excited state grating diffraction efficiency as a function of probe wavelength. A single crystal of 10^{-4} M/M pentacene in p-terphenyl was used. The experimental procedure consisted of maintaining constant excitation conditions, and tuning the probe wavelength through the pentacene $S_0 \rightarrow S_1$ absorption origin. At each of 20 wavelengths, the diffracted intensity was recorded. Transmission was also recorded to measure the absorption strength.

The transient grating experimental setup is illustrated in Fig. 2. The laser is a continuously pumped Nd: YAG system which is acousto-optically mode locked and Q switched to produce high repetition rate (400 Hz), high power infrared (1.06 μm) picosecond pulses. The laser output is a train of about 40 mode-locked pulses, 5.7 ns apart, with ~1.4 mJ total energy. A large pulse from the train is selected by a Pockels cell with avalanche transistor driver. The single pulse is frequency

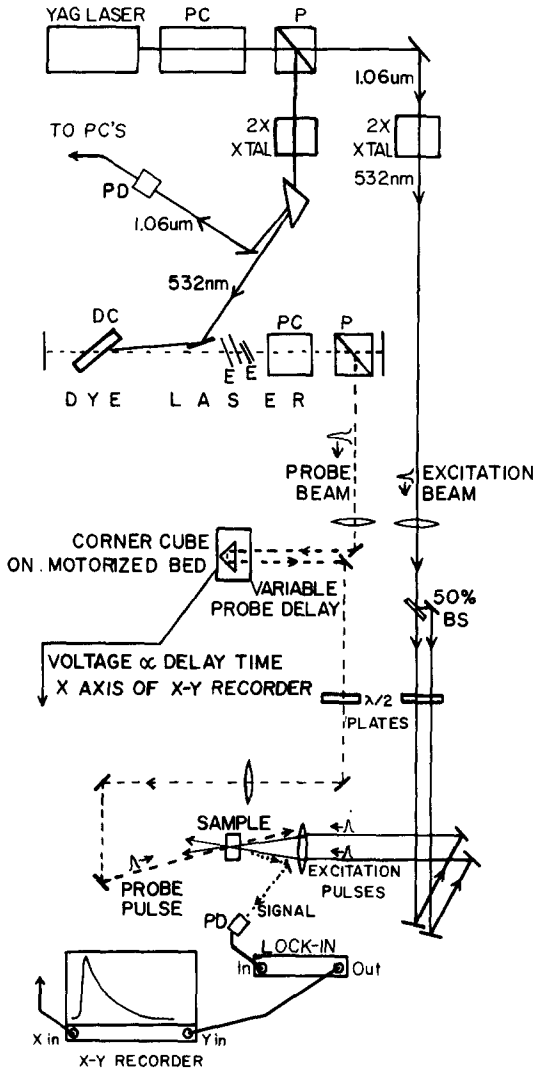

FIG. 2. Transient grating experimental setup. A single 1.06 μm pulse is selected from the YAG mode-locked pulse train and frequency doubled to 532 nm, then split into the two excitation pulses and recombined at the sample to generate the counter-propagating waves and transient grating. The rest of the pulse train is frequency doubled to synchronously pump a tunable dye laser whose output probes the grating after a variable delay. The Bragg-diffracted part of the probe pulse is the transient grating signal. PC ≡ Pockels cell; P ≡ polarizer; PD ≡ photodiode; DC ≡ dye cell; E ≡ etalon; BS ≡ beam splitter.

doubled using CD*A to give a 20 μJ, 80 ps, transform limited, TEM_{00} pulse at 532 nm. This passes through a 50% beam splitter to create the two excitation pulses, which travel equal distances and are focused into the sample.

The unused IR pulse train comes off a reflecting polarizer into another CD*A doubler crystal, and the 532 nm light is used to synchronously pump a dye laser which is spectrally narrowed and tuned by two intracavity etalons. The dye laser is cavity dumped using another Pockels cell with avalanche transistor driver to give an 8 μJ, 30 ps pulse with a spectral width of ~1 cm^{-1}. Synchronization of the two Pockels cells is obtained by a single avalanche transistor which itself is triggered by the IR pulse train. The dye laser output travels a variable distance controlled by a motorized delay line consisting of a corner cube drawn along a precision optical rail. It probes the grating at an angle satisfying the Bragg diffraction condition. The excitation and probe spot sizes were 250 and 150 μm, respectively.

The diffracted signal and transmitted intensity were measured with large area photodiodes and a lock-in amplifier. At all probe wavelengths, the probe pulse was delayed to arrive 500 ps after the excitation pulses. The excitation and probe pulse intensities were kept constant and were filtered to well below saturation levels.

In earlier experiments, the results of which will be displayed in Sec. V, the time dependence of diffracted signal was recorded. In this case, the lock-in amplifier output drives the y axis of an x–y recorder. The x axis is driven by a variable voltage derived from a ten-turn potentiometer connected to the delay line motor, providing the time scale. When the delay line is run, the time-dependent diffracted signal is recorded directly on the x–y recorder.

Pentacene in p-terphenyl samples were obtained by recrystallizing and extensively zone refined (>200 passes) p-terphenyl (Eastman Scintillation Grade), adding various concentrations of pentacene (Aldrich), and growing crystals under vacuum by the Bridgeman technique. A single crystal was cleaved along the $\overline{ab}$ plane to yield a 200 μm thick, high optical quality sample. This was immersed in a cell filled with index-matching fluid (3M Co. FC-43) and used for the experiments.

IV. RESULTS AND DISCUSSION

The wavelength dependence of the pentacene in p-terphenyl excited state grating diffraction efficiency $\eta_{ex}(\omega)$ is plotted in Fig. 3(a). The circles with solid curve show the experimentally measured diffraction, corrected to eliminate the small absorption effects (i.e., diffraction efficiency divided by I/I_0, the ratio of transmitted to incident probe light. This ratio was greater than 0.8 at all wavelengths). The dashed curve shows the theoretically predicted diffraction efficiency from Eq. (19), with no absorption effects. ($D_{av} = 0$. Thus, the dashed curve is identical to the absorption spectrum; see inset). The agreement between the experimentally measured and theoretically predicted diffraction is good, especially on the red side of the origin, which is spectrally isolated. The blue side of the origin is influenced by the next absorption band (see inset spectrum).

It is clear that the diffraction efficiency is not adequately described by amplitude grating effects alone [the dot–dash curve in Fig. 3(a)]. At the absorption peak, the phase contribution vanishes [Eq. (15)], and thus the amplitude contribution η_a, accounts for all of the observed signal. η_a scales as the square of the absorption strength, and the dot–dash curve in Fig. 3(a) was plotted by using the inset absorption spectrum. The difference between this curve and the observed signal gives the diffraction due to phase grating effects. This is plotted

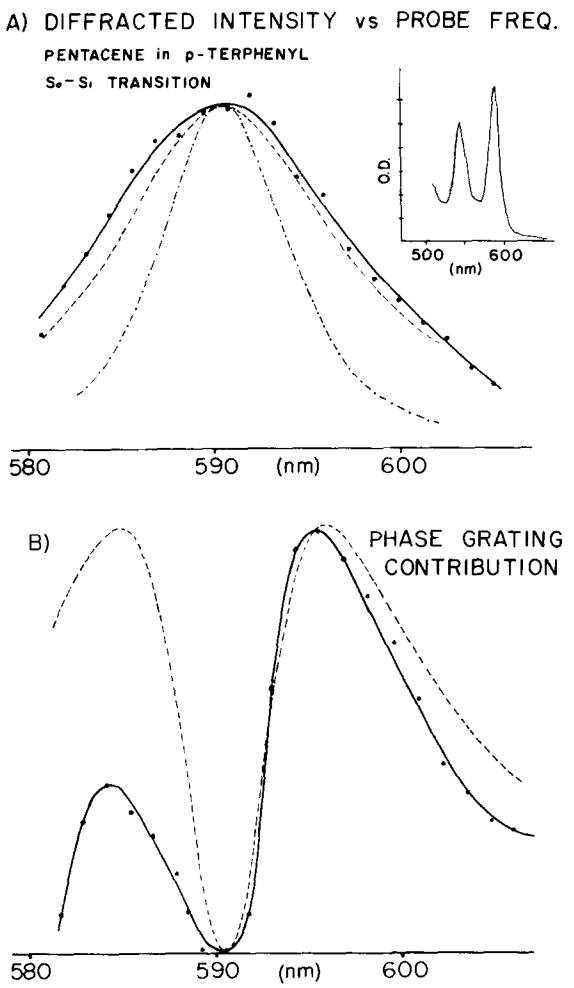

FIG. 3. (a) The circles with the solid line are the experimentally measured excited state grating diffraction intensity as a function of probe wavelength near the S_0–S_1 transition of pentacene in a crystal of p-terphenyl. The dashed curve is theoretically calculated from the absorption spectrum (inset). The dash–dot curve is the calculated amplitude grating contribution to the diffraction efficiency. This demonstrates the significant contribution of phase grating effects. (b) The points with the solid line are the phase grating contribution to the diffraction intensity obtained by subtracting the curves in (a). The predicted m shape curve associated with excited state phase grating diffraction is clearly observed. The dashed curve is theoretically calculated from the absorption spectrum. On the red side where the transition is isolated the agreement is good. On the blue side interference from the next spectral peak (see inset), which was not included in the calculation, influences the dispersion effect.

in Fig. 3(b) (the circles with solid curve). The phase grating contribution rises from zero at the absorption peak to maxima at the half-widths, then gradually decreases, as theoretically predicted (the dashed curve) from Eqs. (6) and (15). The asymmetry in the experimentally measured $\eta_p(\omega)$ is due to the influence of absorption bands on the blue side of the origin which were not included in the calculation.

These results clearly confirm the theoretical prediction of excited state phase grating effects. Although these effects have been discussed by a number of authors, experimental observations have been very few.[16,18] The results presented here may provide the clearest characterization of the wavelength dependence of excited state phase grating diffraction.

V. MIXED EXCITED STATE AND ACOUSTIC GRATING EXPERIMENTS

A. Acoustic phase gratings

Figure 4 shows transient grating data reported earlier from a 10^{-4} M/M pentacene in p-terphenyl crystal.[8] The oscillations on the excited state decay arise from the optical generation of ultrasonic waves which result in a mixed excited state–acoustic grating. This data was taken under conditions similar to those discussed in Sec. III, except that the excitation power was high and substantial, virtually instantaneous heating of the lattice took place during the 80 ps excitation. Due to excited state–excited state absorption, heating is nonlinear. At low excitation power, such as that used in the experiments described above, the lattice is not significantly heated and the data decays smoothly, without modulation. The modulations appear at higher power and increase with power.

The generation of the ultrasonic waves as a result of transient grating excitation has been discussed in detail earlier.[7] It has been shown that counterpropagating acoustic waves of the form

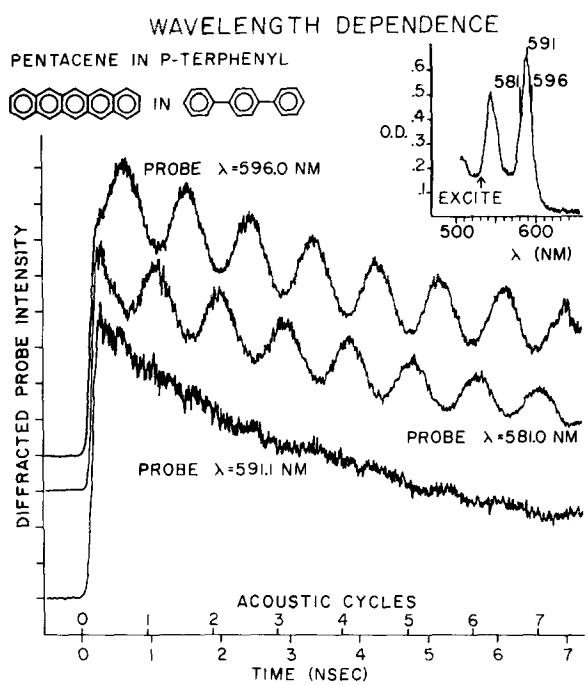

FIG. 4. Mixed excited state–acoustic wave grating probe wavelength dependence. The oscillating component of the signal arising from acoustic waves increases when the probe wavelength is red of the pentacene absorption peak (see inset), decreases when the probe wavelength is blue of the absorption peak, and vanishes when the probe wavelength is at the peak. All experiments were done with identical excitation conditions. This wavelength dependence is due to a combination of acoustic phase grating diffraction (probe wavelength independent), and excited state phase and amplitude grating diffraction (both probe wavelength dependent).

$$S = B\cos Kz(1-\cos\omega_s t) \tag{30}$$

are generated, where S is the strain, K is the acoustic (grating) wave vector ($K=2\pi/\Lambda$, where Λ is the grating fringe spacing defined in Fig. 1), and ω_s is the acoustic frequency ($\omega_s/K=v_s$, the speed of sound). The acoustic amplitude B depends on the excitation power and on sample parameters such as absorptivity, thermal expansion and elastic stiffness coefficients, etc.[7] Ultrasonic waves can also be generated via transient grating-induced stimulated Brillouin scattering (electrostriction). The Brillouin scattering does not involve sample heating.[8,9]

To analyze the mixed transient grating data, we return to Eq. (29) of Sec. II. This gives the diffraction efficiency, assuming that the acoustic effects are limited to phase grating effects due to changes in density. That this is the case will be shown below. By inserting Eq. (30) into Eq. (29), it is apparent that the acoustic diffraction term [the last term in Eq. (29)] has an oscillatory time dependence. The excited state terms decay with the pentacene S_1 state lifetime, $\tau_0\approx 10$ ns, i.e., $N_1(t)=N_1(0)e^{-t/\tau_0}$. Thus, the signal gradually decays and is modulated at the acoustic frequency.

The first two sweeps in Fig. 4 show data taken with probe wavelengths on the red and blue side, respectively, of the absorption peak. In the top sweep, the modulations periodically increase the diffracted signal; in the second sweep, the modulations periodically decrease the diffracted signal. Since the second term in Eq. (29) (the excited state phase grating term) changes sign as the probe frequency passes through the absorption peak ω_0, this behavior is expected. On the red side of the peak, the excited state and acoustic phase grating terms are of the same sign, and, thus, the effect of the acoustic wave is to periodically increase the phase grating contribution and the overall diffraction. On the blue side of the line, the excited state and acoustic phase grating terms are of opposite sign, so the acoustic wave decreases the phase contribution and the overall diffraction.

The bottom sweep in Fig. 4 shows data taken with the probe wavelength at the absorption peak. In this case, the modulations essentially vanish. This is also understood in terms of Eq. (29). At the peak, the second term (excited state phase grating) vanishes. The first term (excited state amplitude grating) is largest at this wavelength, and its square is far greater than the square of the third term (acoustic phase grating). Thus, acoustic effects have negligible effect on the signal.

Also reported earlier were the results of an investigation of mixed grating concentration dependence in pentacene in p-terphenyl.[8] It was found that the data were concentration independent, i.e., amplitudes of modulation relative to the excited state grating signal did not change as crystals of various concentration were tested, keeping all other conditions constant. This is to be expected from Eq. (29), since both $k_0(\omega)$ and ΔS increase linearly with concentration, leaving the relative contributions of the three terms unaffected.

Extensive LIPS data has been presented for this and other mixed crystal systems, pure crystals, glasses, pure liquids, and liquid solutions.[7-9,11] All of the data can now be explained in terms of Eq. (29). The ultrasonic wave grating is, in all cases, a phase grating arising from changes in density of the bulk medium. The interpretation originally put forward was based on an analysis of excited state gratings that included only amplitude grating effects [the first term in Eq. (29)]. The magnitude of the modulations in the room-temperature pentacene in p-terphenyl data was believed to reflect the magnitude of density-dependent spectral shifts, and density-dependent spectral shifts were erroneously reported.[7,8]

In the experiments described above, acoustic wave generation occurs via the absorptive heating mechanism. A detailed theoretical description of electrostrictive coupling (stimulated Brillouin scattering) between the crossed excitation pulses and the material acoustic field showed that electrostrictive ultrasonic wave generation should be possible with transient grating excitation.[8] It is interesting to note that electrostrictive ultrasonic wave generation has since been achieved in transient grating experiments,[9,11] and the theory originally presented was correct. In the presence of strong absorption, as in the pentacene in p-terphenyl experiments discussed here, the absorptive heating mechanism dominates. With the present contribution many aspects of mixed grating experiments are now understood.

B. Relative magnitudes of contributions to diffraction. Possible observation of strain-induced spectral shift acoustic amplitude gratings

In this section, calculations are presented which illustrate the relative magnitudes of the various contributions to diffraction from a mixed excited state and acoustic grating. The terms are listed in Eq. (27). As an example, their values for pentacene in p-terphenyl at room temperature are calculated and used to analyze the data presented in Fig. 4. Other possibilities are then discussed.

From the absorption spectrum of 10^{-4}M/M pentacene in p-terphenyl, $\omega_0=3.2\times10^{15}$ s^{-1}, $\gamma_0=6.0\times10^{13}$ s^{-1}, and $k_0(\omega_0)=2\,|n_0(\omega_0\pm\gamma_0(2)|=1.1\times10^{-4}$; $n_0(\omega\approx\omega_0)=1.58$.[19] This data is for b axis polarized light striking the $\overline{ab}$ crystalline face, as was used for the experiments. The index of refraction is essentially independent of wavelength away from the host resonances. For moderately high excitation power, $N_1/N_0\approx 0.5$ and the maximum strain is $S_{max}\approx 2\times10^{-5}$. For the top two traces in Fig. 4, $|2(\omega_0-\omega)/\gamma_0|\approx 1.0$, and thus the magnitudes of the first two terms in Eq. (29) are each about 2.5×10^{-5}. The third term in Eq. (29) is about 7×10^{-6} at its maximum, and produces significant oscillations in the data. In the third trace in Fig. 4, the first term doubles to 5.0×10^{-5}, the second term vanishes, and the third is unaffected. In this case, since the terms are squared,

the contribution of the first term dominates, and the signal decays essentially without modulation.

The other three terms in Eq. (28) (the second, third, and sixth terms) play no significant role under these conditions. From Eqs. (23), (26), and (25), respectively, their maximum values are

$$\Delta k_s(\omega) = -Sk_0(\omega_0)\,, \tag{31}$$

$$\Delta k_{S'}\left(\omega_0 \pm \frac{\gamma_0}{2\sqrt{3}}\right) = \frac{3\sqrt{3}}{4}\,\phi\Delta S\,\frac{k_0(\omega_0)}{\gamma_0}\,, \tag{32}$$

$$\Delta n_{S'}\left(\omega_0 \pm \frac{\sqrt{3}\,\gamma_0}{2}\right) = \pm\tfrac{1}{4}\,\phi\Delta S\,\frac{k_0(\omega_0)}{\gamma_0}\,. \tag{33}$$

These terms describe the amplitude grating effects of changes in density and the amplitude and phase grating effects of spectral shifts, respectively. In almost all materials for which pressure-dependent spectral shifts have been measured, the shift $\Delta\omega$ lies between 10 and 100 cm^{-1}/kbar, corresponding to $10^{14}\ s^{-1} < \phi < 10^{15}\ s^{-1}$. Even with the upper limit of $\phi = 10^{15}\ s^{-1}$, the terms in Eqs. (32) and (33) are roughly 5.0×10^{-8} and 1.0×10^{-8}, respectively. The term in Eq. (31) is about 2×10^{-9}. These values are negligible compared to the values of the other terms in Eq. (29).

The terms in Eqs. (32) and (33) describe the amplitude and phase grating effects, respectively, of strain-dependent spectral shifts. Measurement of spectral shifts would permit direct calculation of the strengths of excited state phonon and excited state intermolecular interactions in condensed phases. It is thus useful to consider the conditions under which diffraction due to spectral shifts could be observed. From Eqs. (32) and (33), it is clear that stronger absorption, i.e., a larger value of $k_0(\omega_0)$ and narrower linewidths, i.e., a smaller value of γ_0, will make the spectral shift contribution larger. Thus, a sharp and intense transition should show spectral shift affects. For a sample such as pentacene in p-terphenyl, this suggests that at low temperature, spectral shifts could be observed. For example, at 4.2 K the pentacene in p-terphenyl linewidth decreases by about a factor of 100, and the absorption maximum [see Eq. (18)] increases similarly. Thus, the terms in Eqs. (32) and (33) would increase by about 10^4, making spectral shift effects easily observable. It therefore appears that the mixed transient grating technique should be useful for density-dependent spectroscopy. We note that data has been taken at liquid helium temperatures but it is not known yet whether the observed modulations were due to changes in density or to spectral shifts.

VI. CONCLUDING REMARKS

In this paper, a comprehensive analysis of the results of laser-induced grating experiments has been presented. The changes in both real and imaginary parts of the complex index of refraction which occur upon optical excitation have been taken into account. These changes result in phase grating and amplitude grating contributions, respectively, to diffraction from a laser-induced excited state concentration grating. Experimental results have been presented which confirm the theoretical predictions of the wavelength dependence of phase and amplitude grating diffraction.

A detailed analysis of diffraction from laser-induced ultrasonic waves has also been presented and compared to experiment, with special emphasis on diffraction from mixed excited state and acoustic gratings. The conditions under which LIPS experiments could measure strain-induced spectral shifts are also discussed. These experiments are currently in progress.

The time dependence of diffraction from laser-induced excited state gratings is in general unaffected by the analysis presented here. Thus, dynamic information about excited state relaxation, energy transfer, etc., can still be obtained. In experiments in which the absolute intensity or the wavelength dependence of diffraction is analyzed, excited state phase grating effects must be accounted for.

ACKNOWLEDGMENTS

We would like to thank Dr. Marc Pierre, Laboratoire de Spectromé Physique, Université I, 38041 Grenoble, France, for very useful comments pertaining to this work. R. J. D. M. would like to thank the National Sciences and Engineering Research Council of Canada for a postgraduate scholarship. R. C. would like to acknowledge a NATO postdoctoral fellowship. We would also like to thank the National Science Foundation (DMR 79-20380) for support of this research.

[1](a) H. J. Eichler, Opt. Acta 24, 431 (1977); (b) A. von Jena and H. E. Lessing, Opt. Quantum Electron. 11, 419 (1979).
[2]J. R. Salcedo, A. E. Siegman, D. D. Dlott, and M. D. Fayer, Phys. Rev. Lett. 41, 131 (1978).
[3]D. R. Lutz, K. A. Nelson, C. R. Gochanour, and M. D. Fayer, Chem. Phys. 58, 325 (1981).
[4]J. R. Andrews and R. M. Hochstrasser, Chem. Phys. Lett. 76, 207 (1980).
[5]D. W. Phillion, D. J. Kuizenga, and A. E. Siegman, Appl. Phys. Lett. 27, 85 (1975); R. S. Moog, M. D. Ediger, S. G. Boxer, and M. D. Fayer, J. Phys. Chem. (in preparation, 1982).
[6]H. J. Eichler, G. Salje, and H. Stahl, J. Appl. Phys. 44, 5383 (1973).
[7]K. A. Nelson and M. D. Fayer, J. Chem. Phys. 72, 5202 (1980).
[8]K. A. Nelson, D. R. Lutz, M. D. Fayer, and L. Madison, Phys. Rev. B 24, 3261 (1981).
[9]K. A. Nelson, R. J. Dwayne Miller, D. R. Lutz, and M. D. Fayer, J. Appl. Phys. 53, 1144 (1982).
[10]D. W. Pohl and V. Irniger, Opt. Commun. 18, 149 (1976); Phys. Rev. Lett. 36, 480 (1976).
[11]R. J. Dwayne Miller, R. Casalegno, K. A. Nelson, and M. D. Fayer, Chem. Phys. (in preparation, 1982).
[12]A. E. Siegman, J. Opt. Soc. Am. 67, 545 (1977).
[13]H. Kogelnik, Bell Syst. Tech. J. 48, 2909 (1969); R. Collier, L. B. Burkhardt, and L. H. Lin, *Optical Holography* (Academic, New York, 1971).
[14]R. S. Longhurst, *Geometrical and Physical Optics*, 2nd ed. (Wiley, New York, 1967); C. J. F. Bottcher, *Theory of Electric Polarization* (Elsevier, Amsterdam, 1952); M. Born and K. Huang, *Dynamical Theory of Crystal Lattices* (Clarendon, Oxford, 1954).

[15]A. C. G. Mitchell and M. W. Zemansky, *Resonance Radiation and Excited Atoms* (Cambridge University, Cambridge, 1961).
[16]G. E. Scrivener and M. R. Tubbs, Opt. Commun. **10**, 32 (1974).
[17]A. Yariv, *Quantum Electronics*, 2nd ed. (Wiley, New York, 1975).
[18]W. J. Tomlinson, E. A. Chandross, R. L. Fork, C. A. Pryde, and A. A. Lamola, Appl. Opt. **11**, 533 (1972); W. J. Tomlinson and G. D. Aumiller, *ibid.* **14**, 1100 (1975); A. V. Alekseev-Popov, N. G. Dyachenko, V. E. Mandel and A. V. Tyurin, Opt. Spectrosc. **47**, 323 (1979).
[19]A. N. Winchell, *The Optical Properties of Organic Compounds*, 2nd ed. (Academic, New York, 1954).